Indian Journal of Pure & Applied Physics
Vol. 62, August 2024, pp. 689-699
DOI: 10.56042/ijpap.v62i8.8432

Spectral Class Transition of GRO J1655-40 during 2005 outburst in the Light of TCAF Model

Md Washimul Bari[a,b] & Achintya Kumar Chatterjee[b*]

[a]Department of Physics, Adamas University, Adamas Knowledge City, Barasat, Kolkata-700 126, West Bengal, India

[b]Indian Centre for Space Physics, 466 Barakhola, Netai Nagar, Kolkata-700 099, West Bengal, India

Received 31 January 2024; accepted 1 July 2024

Galactic transient black hole candidates often show notable changes in their X-ray properties during outbursts. In this paper we study the timing and spectral properties of the transient X-ray binary GRO J1655-40 during its 2005 outburst using the Two Component Advective Flow (TCAF) model as a local model in *XSPEC*. We analyze the data of PCA onboard the Rossi X-ray Timing Explorer (RXTE) satellite from February to October 2005. Here we present a detailed insight in to the mass accretion mechanism and the characteristics of the accretion disk around the black hole candidate throughout the period of outburst. Based on the TCAF model fitting, parameters of the accretion flow *e.g.*, the Keplerian rate or disk rate, sub-Keplerian rate or halo rate, shock location and the compression ratio or the shock strength are derived. On the basis of the evolution of the accretion rate ratio (*ARR*) or the ratio of the halo rate to the disk rate and considering the presence or absence of the Quasi-Periodic Oscillations (QPOs), we have categorized the entire outburst into four distinct spectral states: hard, hard-intermediate, soft-intermediate, and soft. It reveals that these distinct spectral states form a characteristic q-like pattern or hysteresis loop following the sequence: hard – hard-intermediate – soft-intermediate – soft – soft-intermediate – hard-intermediate – hard. We find that during the rising or declining phases, where the QPO frequencies are increasing or decreasing respectively, there is an associated rise in the value of the halo rate compared to the disk rate. We have also observed that the *ARR* reaches its maximum on the day of transition from the hard state to the hard-intermediate state during the rising phase, and on the day of transition from the hard-intermediate state to the hard state during the declining phase.

Keywords: X-Rays; Binaries–stars individual; (GRO J1655-40)–stars; Black holes–accretion; Accretion disks – spectrum – radiation; Dynamics

1 Introduction

During outbursts galactic transient black hole (BH) candidates exhibit interesting evolutions in timing and spectral properties in X-rays. Several workers[1-5] reported the temporal and spectral evolutions of the transient black hole binaries during their outbursts. Several spectral states have been identified as the BH candidate goes through different outburst phases. Generally, four basic spectral states are found in spectral evolution of black hole candidates – hard, hard-intermediate, soft-intermediate and soft states. The spectral states are observed to form a q-like pattern or a hysteresis loop during the outbursts[4,6-8] which is nothing but an X-ray hardness-intensity diagram plotted in the log-log scale. One of the unique features that reveals from the temporal analysis of the X-ray variations during the outburst is the evolution in the power density spectrum (PDS). The different components of a PDS[9,10] are – a flat-top component, a break frequency and a power-law like distribution etc. with a quasi-periodic oscillation (QPO). X-ray transient sources primarily exhibit soft and hard spectral states during their outbursts[5,11,12] and the PDSs are substantially different in two spectral states – hard state pertaining to flatter PDS and soft state pertaining to steeper PDS. Several workers[13-20] also reported the evidence of state transition of other compact objects.

GRO J1655-40 is a well-known transient X-ray binary having undergone several major outbursts. It was discovered[21,22] in 1994 by the BATSE (Burst and Transient Source Experiment) instrument onboard the Compton Gamma Ray Observatory. This low mass X-ray binary (LMXB), located at a distance[23] of 3.2 ± 0.2 *kpc*, consists of a 7.02 ± 0.22 $M_{\odot}$ black hole[24] which orbits a companion star[25,26] of mass 2.3 $M_{\odot}$ in 2.62 day. The disk is inclined[24] at an angle of $69.5^{\circ} \pm 0.1^{\circ}$ approximately. The Rossi X-ray Timing Explorer (RXTE) mission extensively observed the source during 1996-1997 when it was active in X-rays for 16 months and showed a complex timing and spectral behaviour. After that it

*Corresponding author: (E-mail: akcmalda@gmail.com)

remained in quiescent state for more than 7 years until a rise in the X-rays flux was detected[27-29] by RXTE/PCA in February 2005. The source was again extensively observed by RXTE and it was found to remain active in X-rays for about 260 days. In this present paper, we provide the result of timing and spectral analysis of RXTE/PCA data of the source GRO J1655-40 obtained from NASA archive (*https://heasarc.gsfc.nasa.gov/*) during 2005 outburst. We have analyzed a total of 240 days data from February 25, 2005 to October 22, 2005. We analyze the PCA spectra using two-component advective flow (TCAF) solution as a local model of XSPEC. The TCAF model requires two accretion rates - the Keplerian disk accretion rate and the halo accretion rate. The latter is composed[30,31] of a sub-Keplerian, low angular momentum flow which may or may not develop a shock. Based on the accretion rates, hardness intensity and other parameters, we find that the 2005 outburst of GRO J1655-40 is divided into four spectral states - hard, hard-intermediate, soft-intermediate and soft, in the sequence of hard → hard-intermediate → soft-intermediate → soft → soft-intermediate → hard-intermediate → hard. We got QPOs in the hard and hard-intermediate states both in the rising and declining phases.

Chakrabarti *et al.*[28] reported the propagating oscillatory shock model for QPOs in GRO J1655-40 during the rising phase of its 2005 outburst. Some workers[32,33] reported the 2005 outburst of GRO J1655-40 using Swift and XMM-Newton & INTEGRAL data. Debnath *et al.*[3] presented the results of timing and spectral analysis of RXTE data of the outburst using black body and power-law components in XSPEC wherein they divided the entire episode of the outburst in four spectral states viz. hard, soft, very soft and intermediate. Aktar *et al.*[34] employed GRO J1655-40 data obtained from RXTE during the 1996 outburst for studying the advective flow properties around rotating black holes. Here, in this paper we present the result of temporal and spectral analysis of RXTE data of outburst of GRO J1655-40 during 2005 using different energy range compared to other workers. Most importantly, we have done the spectral analysis using Two-Component Advective Flow (TCAF) solution as a local model in XSPEC[35] for a better understanding of the accretion flow dynamics and transition from one spectral state to another during the 2005 outburst of GRO J1655-40.

2 Observation and Data Analysis

We present the result of analysis of publicly available data in the archive from the Proportional Counter Array (PCA) instrument of Rossi X-ray Timing Explorer (RXTE) of the 2005 outburst of GRO J1655-40. We analysed the RXTE data from 25 February 2005 (Modified Julian Date or MJD 53426) to 22 October 2005 (MJD 53665) from the PCA. We carry out our data analysis using FTOOLS software package Heasoft version HEADAS-6.10 and XSPEC version 12.6. For the overall study of spectral and timing properties of the source, we followed the analysis described in Debnath *et al.*[35,36]. We extracted data from PCU2, the most stable and well-calibrated proportional counter unit. We extracted the light curves using *saextrct* task for science array data. To generate the power-density spectra (PDS), we utilized the *powspec* task from the XRONOS package, applying a normalization factor of '-2' to subtract the expected 'white' noise RMS fractional variability from the light curves pertaining to 0-35 channels of PCU2 with bin size of 0.01 *second*. We extracted the PCA background using the *runpcabackest* command and the latest bright-source background model. To account for data from the South Atlantic Anomaly (SAA), we incorporated the PCA SAA history file. The 2.5-25 keV PCA spectra from these observation IDs underwent appropriate background subtraction and were fitted with a TCAF solution-based additive model fits file *TCAF_v0.1_R3.fits*.

2.1 Light Curve and Hardness Ratio

For studying the X-ray intensity variations of the 2005 outburst of GRO J1655-40, we extracted light curves from PCA data acquired by the RXTE/PCA instrument in the different energy bands 5–8 keV (11–19 channels), 9–15 keV (20–35 channels), and 5–15 keV (11–35 channels). We divided the 5–15 keV energy band into the above two bands because the 5–8 keV photons mainly come from a thermally cool Keplerian disk, whereas the photons in the higher energy band (9–15 keV) come from a Comptonized sub-Keplerian disk. However, this may not necessarily be true always because the contributions for different spectral components also depend on accretion states. We have extracted light curves using the *FS37*.gz* file in which data is available up to 35 channels corresponding to maximum energy of 15 keV.

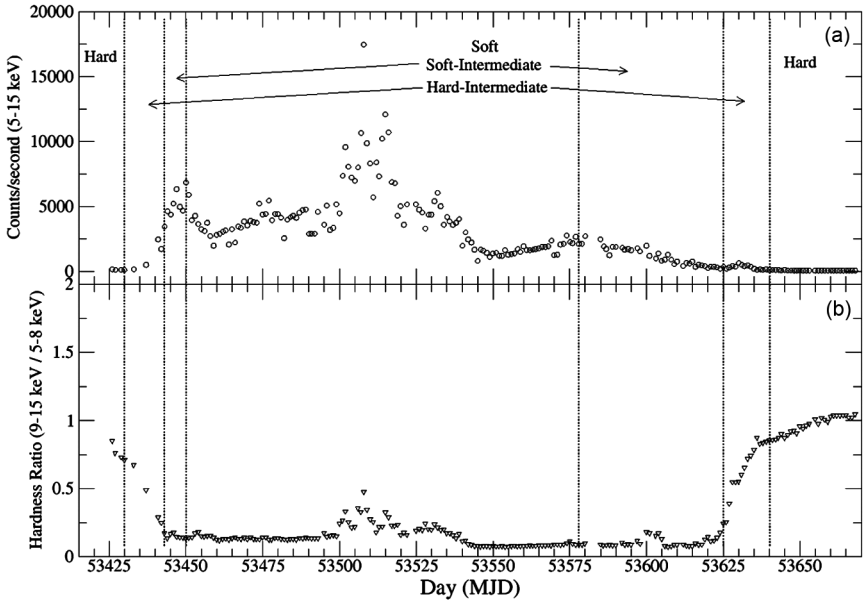

Fig. 1 — (a) 5–15 keV PCA count rate (Counts/second) and (b) hardness ratio (ratio of the photon count rates in the 9–15 keV to 5–8 keV bands) as a function of the MJD during the 2005 outburst of GRO J1655-40. The vertical dashed lines indicate transition of spectral states

In Fig. 1(a&b) the total 5-15 keV PCA count rate (Counts/second) and the hardness ratio (ratio of the photon count rates in the 9–15 keV to 5–8 keV bands) are plotted against MJD. The hard to hard-intermediate state transition took place on 1 March 2005 (MJD 53430), the hard-intermediate to soft-intermediate transition on 14 March 2005 (MJD 53443), the soft-intermediate to soft transition on 21 March 2005 (MJD 53450), the reverse transition from the soft to soft-intermediate state on 27 July 2005 (MJD 53578), the soft-intermediate to hard-intermediate state transition on 12 September 2005 (MJD 53625), and finally on 27 September 2005 (MJD 53640) hard-intermediate to hard state transition occurred. These state transitions are indicated by vertical dotted lines in the figure. Rapid changes in the hardness ratio are seen (Fig. 1(b)) in the hard and hard-intermediate states, whereas in the soft and soft-intermediate states the hardness ratio changes very slowly. The hard and hard-intermediate states are represented by both the falling and rising arms of the hardness ratio in the outburst profile and we found QPOs in these states. This scheme of classification of spectral states confirms the previous observation of Debnath *et al.*[3],who used a slightly different energy range.

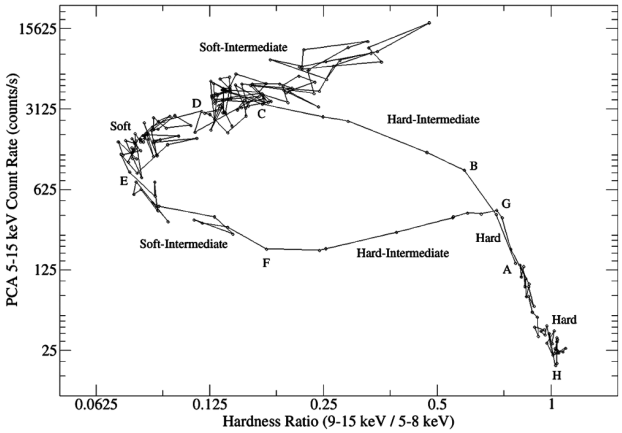

Fig. 2 -Hardness Intensity Diagram of GRO J1655-40 observed with RXTE/PCA during its 2005 outburst as it approaches the soft state from the hard state via hard-intermediate and soft-intermediate spectral states. The total count rates in the 5–15 keV energy band are shown along Y-axis and the ratio of the count rates in the 9–15 keV and 5–8 keV bands are given on the X-axis. The points A, B, C, D, E, F and G correspond to MJD 53426, MJD 53430, MJD 53443, MJD 53450, MJD 53578, MJD 53625, MJD 53640 and MJD 53665 respectively

2.2 Hardness Intensity Diagram

We plotted the Hardness Intensity Diagram (HID) to study the evolution of timing and spectral properties during the 2005 outburst of GRO J1655-40. In Fig. 2, we plotted the PCA 5–15 keV count rate as a function of Hardness Ratio defined by the ratio of the flux in the 9–15 keV to that in the 5–8 keV energy band on logarithmic scale. The point A indicates the start and the point H indicates the end of the RXTE observations respectively, whereas the points B, C, D, E, F, and G are the points which indicate state transitions from hard to hard-intermediate, hard-intermediate to soft-intermediate, soft-intermediate to soft, soft to soft-intermediate, soft-intermediate to hard-intermediate and hard-intermediate to hard

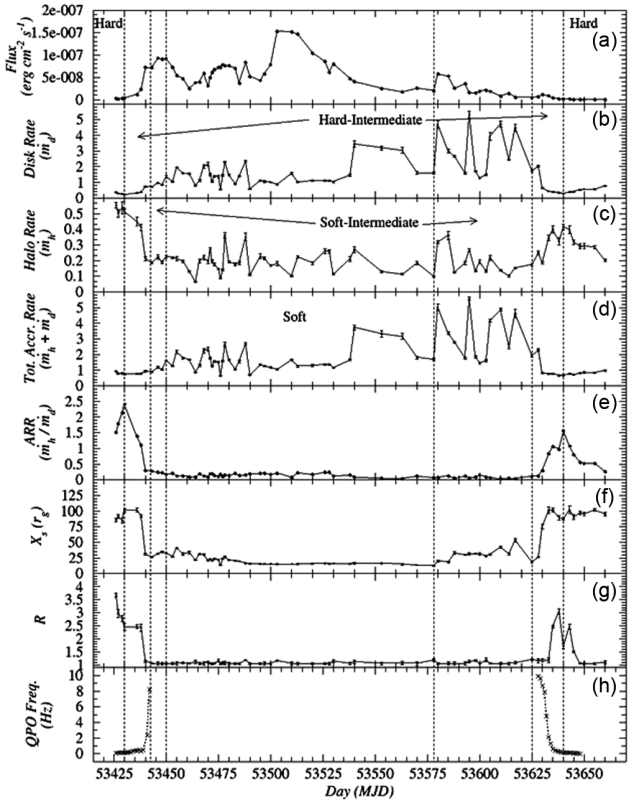

Fig. 3 — Variation of (a) flux and TCAF model fitted (b) Keplarian rate or disk rate $\dot{m}_d$, (c) the sub-Keplarian rate or halo rate $\dot{m}_h$, (d) total accretion rate ($\dot{m}_d + \dot{m}_h$), (e) ARR (*i.e.*, ratio between the halo and disk rates), (f) shock location (X_s), (g) compression ratio (R) and (h) observed QPO frequency in Hz with day (MJD) for the 2005 outburst of GRO J1655-40 are shown. Vertical dashed lines indicate the points where transitions between different spectral states are believed to occurs

respectively. A detailed physical picture is discussed in the next section.

We observed that the pre- and post-outburst phases appear and disappear from the low photon count region attributed to the harder spectrum. The hardness ratio changed rapidly in the hard state compared to soft and intermediate states.

2.3 Quasi Periodic Oscillation

From the initial day (25 February 2005) of RXTE/PCA observation the source was in hard state and we observed a QPO of frequency of 0.082 *Hz* on the very first day. Variations of QPO frequencies with time (MJD) during the rising and declining phases are shown in Fig. 3(h). The QPO frequency increased gradually all through the hard-intermediate state where it reached to 8.2 *Hz* on 13 March 2005. The source moved to soft-intermediate spectral state on 14 March 2005. No QPO was observed in the soft-intermediate and soft states.

Table 1 — Observed QPO Frequencies & Q-factors

MJD	Date	QPO Frequency (*Hz*)	Q-factor
	Rising Phase		
53426	25-02-2005	0.082	21.683
53427	26-02-2005	0.114	18.377
53428	27-02-2005	0.119	11.495
53429	28-02-2005	0.131	15.819
53430	01-03-2005	0.106	33.123
53431	02-03-2005	0.131	16.058
53432	03-03-2005	0.161	20.443
53433	04-03-2005	0.168	24.697
53434	05-03-2005	0.304	13.275
53435	06-03-2005	0.368	24.487
53436	07-03-2005	0.402	8.982
53437	08-03-2005	0.479	12.653
53438	09-03-2005	0.311	27.811
53439	10-03-2005	0.455	12.909
53441	12-03-2005	2.349	10.486
53442	01-03-2005	8.205	29.396
	Declining Phase		
53628	15-09-2005	9.906	15.842
53629	16-09-2005	9.620	12.806
53630	17-09-2005	8.710	14.335
53631	18-09-2005	7.884	12.957
53632	19-09-2005	4.792	6.118
53633	20-09-2005	2.110	4.100
53634	21-09-2005	1.274	5.657
53635	22-09-2005	0.599	5.433
53636	23-09-2005	0.421	15.595
53637	24-09-2005	0.314	21.140
53638	25-09-2005	0.228	8.832
53639	26-09-2005	0.196	19.884
53640	27-09-2005	0.140	7.934
53641	28-09-2005	0.131	6.180
53642	29-09-2005	0.105	21.301
53643	30-09-2005	0.102	20.081
53644	01-10-2005	0.091	29.026
53645	02-10-2005	0.041	16.070
53646	03-10-2005	0.023	17.422
53647	04-10-2005	0.045	24.247
53648	05-10-2005	0.012	27.184

The object entered the hard-intermediate state on 12 September 2005 and again in this state we observed QPO of frequency 9.9 *Hz* on 15 September 2005. After that QPO frequency monotonically decreased till the source entered into the hard-spectral state. In the hard state few low frequency QPOs were observed. Due to decrease in photon flux and a lack of long duration observations, low-frequency QPOs were not detected prominently after that. The observed QPO frequencies and the corresponding Q-factors are shown in Table 1.

3 Results of Spectral Analysis using TCAF Model

We fitted the 2.5-25 keV PCA background-subtracted spectra with the TCAF-based model fits file used as a local model in XSPEC. To achieve the best fit we used a *Gaussian* line of peak energy around 6.5 keV (iron-line emission) and *powerlaw*. We kept the hydrogen column density (N_H) fixed at $0.75\times10^{22} atoms\ cm^{-2}$ for the absorption model wabs[37] and considered a systematic error of 1.0 %. For fitting the spectrum with TCAF model we supplied six input parameters: (i) Keplerian rate ($\dot{m}_d$ in Eddington rate), (ii) sub-Keplerian rate ($\dot{m}_h$ in Eddington rate), (iii) black hole mass (M_{BH} in solar mass unit $M_\odot$), (iv) location of the shock (X_s in Schwarzschild radius $r_g = 2GM_{BH}\ c^2$), (v) compression ratio of the shock ($R = \rho_+ / \rho_-$ where ρ_+ and ρ_- are the densities of the post and pre shock matters), and (vi) the model normalization value (*norm*) equivalent to $\frac{1}{4\pi D^2} cos\ (i)$, where D is the source distance in 10 *kpc* unit and i is the disk inclination angle.

Figure 3 shows the variations of flux, QPO and the model fitted parameters. In Fig. 3(a) the variation of flux in the energy range of 2.5-25 keV with MJD is shown. The variations of Keplerian rate or disk rate $\dot{m}_d$, the sub-Keplerian rate or halo rate $\dot{m}_h$ and the total accretion rate with MJD during the observation period are shown in Fig. 3(b-d) respectively. The variation of accretion rate ratio (ARR), defined as the ratio of sub-Keplerian halo rate $\dot{m}_h$ and Keplerian disk rate $\dot{m}_d$, is shown in Fig. 3(e-g) show the variations of TCAF model parameters – shock location (X_s) and compression ratio (R) respectively. The values of the TCAF model fitted parameters are shown in Table 2. As mentioned earlier, observed QPO frequencies are shown in Fig. 3(h). Four different spectral states, *i.e.*, Hard State (HS), Hard-Intermediate State (HIMS), Soft-Intermediate State (SIMS), and Soft State (SS), could be identified during the entire outburst of GRO J1655-40, depending on the variation of these parameters.

Table 2 — TCAF Model Fitted Parameters for 2.5–25 keV

Obs. ID	Date	MJD	$\dot{m}_d$ ($\dot{M}_{Edd}$)	$\dot{m}_h$ ($\dot{M}_{Edd}$)	ARR	X_s (r_g)	R	Reduced χ^2
A-01-01-00	25-02-2005	53426	0.367	0.554	1.510	85.952	3.682	0.733
A-01-01-01	26-02-2005	53427	0.281	0.501	1.783	91.348	2.971	0.655
A-01-01-02	28-02-2005	53429	0.251	0.537	2.139	84.563	2.781	2.148
A-01-01-05	01-03-2005	53430	0.213	0.513	2.408	101.124	2.455	2.046
B-01-01-00	07-03-2005	53436	0.325	0.45	1.385	101.431	2.461	0.463
B-01-01-04	09-03-2005	53438	0.371	0.412	1.111	92.16	2.427	0.501
B-01-02-00	11-03-2005	53440	0.724	0.213	0.294	31.241	1.139	0.312
B-01-03-00	14-03-2005	53443	0.695	0.185	0.266	26.213	1.051	0.642
B-01-05-01	17-03-2005	53446	0.959	0.223	0.233	31.513	1.052	1.337
B-01-07-00	19-03-2005	53448	0.835	0.189	0.226	34.811	1.05	1.042
B-01-09-01	21-03-2005	53450	1.369	0.226	0.165	32.598	1.051	1.241
B-01-12-02	24-03-2005	53453	1.043	0.218	0.209	27.211	1.052	2.243
B-01-14-00	26-03-2005	53455	1.952	0.213	0.109	40.845	1.056	2.682
B-01-16-00	29-03-2005	53458	1.579	0.195	0.123	31.118	1.086	2.153
B-01-19-00	01-04-2005	53461	1.552	0.131	0.084	34.121	1.061	2.772
B-01-22-00	04-04-2005	53464	0.795	0.064	0.081	21.421	1.118	2.531
B-01-24-00	06-04-2005	53466	1.101	0.198	0.180	31.412	1.051	2.724
B-01-26-00	08-04-2005	53468	2.011	0.219	0.109	30.354	1.057	2.127
B-01-27-02	10-04-2005	53470	2.169	0.192	0.089	21.241	1.112	1.950
B-01-29-00	11-04-2005	53471	1.501	0.268	0.179	23.112	1.058	1.277
B-01-29-02	12-04-2005	53472	1.052	0.195	0.185	21.085	1.052	2.035
B-01-31-02	13-04-2005	53473	1.379	0.175	0.127	23.564	1.055	2.634
B-01-32-00	15-04-2005	53475	1.375	0.146	0.106	22.157	1.168	1.894
B-01-33-00	16-04-2005	53476	0.544	0.088	0.162	13.785	1.052	1.987
B-01-34-00	17-04-2005	53477	1.441	0.141	0.098	24.054	1.074	2.105
B-01-34-01	18-04-2005	53478	2.294	0.362	0.158	26.742	1.083	2.054
B-01-36-01	20-04-2005	53480	1.467	0.192	0.131	21.621	1.051	2.255

(*Contd.*)

Table 2 — TCAF Model Fitted Parameters for 2.5–25 keV (*Contd*.)

Obs. ID	Date	MJD	$\dot{m}_d$ ($\dot{M}_{Edd}$)	$\dot{m}_h$ ($\dot{M}_{Edd}$)	ARR	X_s (r_g)	R	Reduced χ^2
B-01-38-00	23-04-2005	53483	0.885	0.176	0.199	20.274	1.052	1.372
B-01-40-00	25-04-2005	53485	1.381	0.184	0.133	19.452	1.055	1.421
B-01-42-00	28-04-2005	53488	2.345	0.351	0.150	16.556	1.181	2.426
B-01-44-00	30-04-2005	53490	0.579	0.109	0.188	15.821	1.051	2.184
B-01-48-00	05-05-2005	53495	1.112	0.227	0.204	15.521	1.052	0.957
B-01-50-00	07-05-2005	53497	1.041	0.213	0.205	15.321	1.051	2.138
B-01-52-02	10-05-2005	53500	1.001	0.168	0.168	15.412	1.050	1.495
B-01-55-00	13-05-2005	53503	0.860	0.181	0.210	15.162	1.161	1.896
B-01-60-00	20-05-2005	53510	1.556	0.102	0.066	15.224	1.054	2.054
B-01-61-02	23-05-2005	53513	1.018	0.223	0.219	15.432	1.051	2.541
B-01-66-02	30-05-2005	53520	1.101	0.184	0.167	15.912	1.052	2.689
B-01-72-01	05-06-2005	53526	1.102	0.261	0.237	16.513	1.051	2.218
B-01-73-02	07-06-2005	53528	1.102	0.259	0.235	15.610	1.050	1.059
B-01-73-01	09-06-2005	53530	1.034	0.113	0.109	16.112	1.15	2.084
B-01-83-04	17-06-2005	53538	1.448	0.211	0.146	15.612	1.051	2.105
B-01-84-00	19-06-2005	53540	3.445	0.271	0.079	16.498	1.122	1.918
B-01-95-02	02-07-2005	53553	3.185	0.129	0.041	16.614	1.055	1.598
B-01-06-10	12-07-2005	53563	3.037	0.113	0.037	14.689	1.071	1.488
B-01-12-12	19-07-2005	53570	1.615	0.185	0.115	13.523	1.051	1.794
B-01-19-10	27-07-2005	53578	1.593	0.098	0.062	12.368	1.189	1.430
B-01-21-10	29-07-2005	53580	4.704	0.318	0.068	20.058	1.052	2.874
B-01-25-11	03-08-2005	53585	3.002	0.361	0.120	18.287	1.051	2.153
B-01-28-10	06-08-2005	53588	2.652	0.124	0.047	32.912	1.055	1.491
B-01-32-10	11-08-2005	53593	1.585	0.185	0.117	29.987	1.051	1.435
B-01-33-12	13-08-2005	53595	5.320	0.267	0.050	31.512	1.128	1.439
B-01-34-10	16-08-2005	53598	1.712	0.135	0.079	31.895	1.17	2.424
B-01-35-10	18-08-2005	53600	1.273	0.193	0.152	31.354	1.054	0.358
B-01-40-10	21-08-2005	53603	1.479	0.132	0.089	27.874	1.187	2.154
B-01-40-11	23-08-2005	53605	3.942	0.219	0.056	30.712	1.062	2.121
B-01-46-12	28-08-2005	53610	4.725	0.137	0.029	41.878	1.051	2.130
B-01-49-11	01-09-2005	53614	2.434	0.101	0.041	31.611	1.050	2.199
B-01-51-12	04-09-2005	53617	4.475	0.152	0.034	53.345	1.080	1.879
B-01-74-02	12-09-2005	53625	1.732	0.173	0.100	18.312	1.199	1.030
B-01-76-00	15-09-2005	53628	2.030	0.249	0.123	26.324	1.161	1.101
B-01-79-00	17-09-2005	53630	0.621	0.184	0.296	75.321	1.181	0.440
B-01-81-00	20-09-2005	53633	0.415	0.345	0.831	101.142	1.180	0.895
B-01-81-02	22-09-2005	53635	0.375	0.399	1.064	101.689	2.465	0.868
B-01-86-00	25-09-2005	53638	0.332	0.323	0.973	89.254	3.058	0.930
B-01-87-00	27-09-2005	53640	0.265	0.414	1.562	87.212	1.729	0.787
B-01-88-00	30-09-2005	53643	0.372	0.397	1.067	101.886	2.471	0.453
B-01-88-01	02-10-2005	53645	0.396	0.317	0.801	90.454	1.510	0.596
B-01-88-05	05-10-2005	53648	0.521	0.291	0.559	97.102	1.051	0.584
B-01-37-10	07-10-2005	53650	0.557	0.292	0.524	95.251	1.050	0.435
B-01-36-10	12-10-2005	53655	0.548	0.285	0.520	101.642	1.050	0.513
B-01-43-12	17-10-2005	53660	0.771	0.202	0.262	94.987	1.101	0.686

Note: Here A = 90428, B = 91702.

3.1 Hard State in the Rising Phase

GRO J1655-40 was found to be in hard state during the first five days (from MJD 53426 to 53430) of its observation by RXTE in 2005. It is clearly evident from the fact that the halo rate is increasing faster than the disk rate during this time. This is because at this stage the in fall time of the sub-Keplerian flow is shorter than that of the Keplerian flow. It is interesting to note that the accretion rate ratio (ARR) exhibits a continuous upward trend and peaked at 2.4 which is the highest point during the entire outburst. As the TCAF model suggests, the shock location (X_s) is seen to be far away (about a hundred Schwarzschild radius) from the black hole. In the initial phase of the hard state, the post-shock matter is seen to be 3.7 times denser than the pre-shock matter. As time goes on, R decreases over time. The QPO frequencies show a consistent, monotonic increase, ranging from 0.082 *Hz* to 0.106 *Hz*. We define the day of maximum halo rate and maximum *ARR*, MJD 53430, as the day on which GRO J1655-40 undergoes transition from hard spectral state to hard-intermediate spectral state.

3.2 Hard-Intermediate State in the Rising Phase

For the next 13 days the object was in Hard-Intermediate State. The halo rate begins to decrease as a part of the sub-Keplerian matter starts converting into Keplerian matter due to viscous effects. So, the disk rate starts rising resulting in a gradual decrease in ARR. The shock location (X_s) starts moving towards the black hole. During this HIMS QPO frequency increases monotonically from 0.13 *Hz* to 8.2 *Hz*. The HIMS ends on MJD 53443 after which ARR and compression ratio become almost constant.

3.3 Soft-Intermediate State in the Rising Phase

The SIMS corresponds to a rise in total accretion rate and PCA count rate, although ARR and R remain almost constant. The peak in PCA rate on MJD 53450 marks the transition of the source from soft-intermediate state to soft state. During the SIMS no QPOs are seen. The shock location is very near the black hole, and its oscillation has stopped during this period due to the rapid cooling of the disk, resulting in the non-fulfilment of the resonant oscillation condition.

3.4 Soft State

For the next 128 days (up to MJD 53578) the source is observed in the soft state. During this period the Keplerian matter supply is higher than that of accretion of sub-Keplerian matter and the spectra are mostly dominated by thermal photons. The PCA count rate becomes considerably high in this state. The shock is in close proximity to the black hole, yet it remains static since the conditions required for resonance oscillation are not met due to rapid cooling. Consequently, the Quasi-Periodic Oscillation (QPO) is not observed. The compression ratio (R) remains nearly equal to 1 throughout. The Keplerian and sub-Keplerian matters are continuously drained out resulting in decrease in PCA rate and flux in the later stage while keeping ARR almost constant. After MJD 53578 the shock location (X_s) starts moving from the black hole indicating transition of the object from soft state to soft-intermediate state.

3.5 Soft-Intermediate State in the Declining Phase

The object was observed in the Soft-Intermediate state for the next ~47 days. In this state, the total accretion rate rises, though the accretion rates are seen to be fluctuating. The accretion rate ratio (ARR) remains almost constant. Whereas the compression ratio shows an increasing tendency only at a later stage. The shock location gradually moves away from the black hole. The PCA rate and flux decrease monotonically. After MJD 53625 the halo rate starts rising and the Keplerian rate starts diminishing sharply showing clearly the transition from Soft-Intermediate state to Hard-Intermediate state.

3.6 Hard-Intermediate State in the Declining Phase

In this state, the depletion of matter reaches a level sufficient to reinstate the resonance state for the oscillation of the Centrifugal pressure supported Boundary Layer (CENBOL), leading to the resurgence of Quasi-Periodic Oscillations (QPOs). The location of the shock (X_s), i.e., the outer layer of CENBOL, started receding rapidly after MJD 53625, because of drop in flow pressure. This, in turn, causes the QPO frequency drop monotonically from 9.9 *Hz* to 0.14 *Hz*. The post-shock matter becomes denser steadily, which is clear from the variation of R. It is evident that the Keplerian rate, or the disk rate, undergoes a rapid decline while the sub-Keplerian halo rate steadily increases, causing a sharp ascent in the accretion rate ratio (ARR). On MJD 53640, the highest Accretion Rate Ratio (ARR) of 1.55 is noted during the declining phase, marking the transition day from the Hard-Intermediate State (HIMS) to the Hard State (HS).

3.7 Hard State in the Declining Phase

During this state, the Accretion Rate Ratio (ARR) undergoes a steady decline from 1.55 to 0.25, while

the observed Quasi-Periodic Oscillations (QPOs) also exhibit a monotonic decrease from 0.14 *Hz* to 0.0115 *Hz*. Notably, despite the opposing trends in disk rate and halo rate—with the former increasing and the latter decreasing—the overall accretion rate remains relatively constant, resembling the pattern observed during the rising phase. The initiation of the rising phase was observed several days after its onset. Throughout the declining phase, observations persisted until the PCA count significantly dropped below that of the first day of the rising phase. The end of the Hard State (HS) marks the conclusion of the outburst.

Figs. 4(a-f) present the background-subtracted PCA spectra in the 2.5-25 keV range, fitted using the TCAF model with variations in χ across three distinct

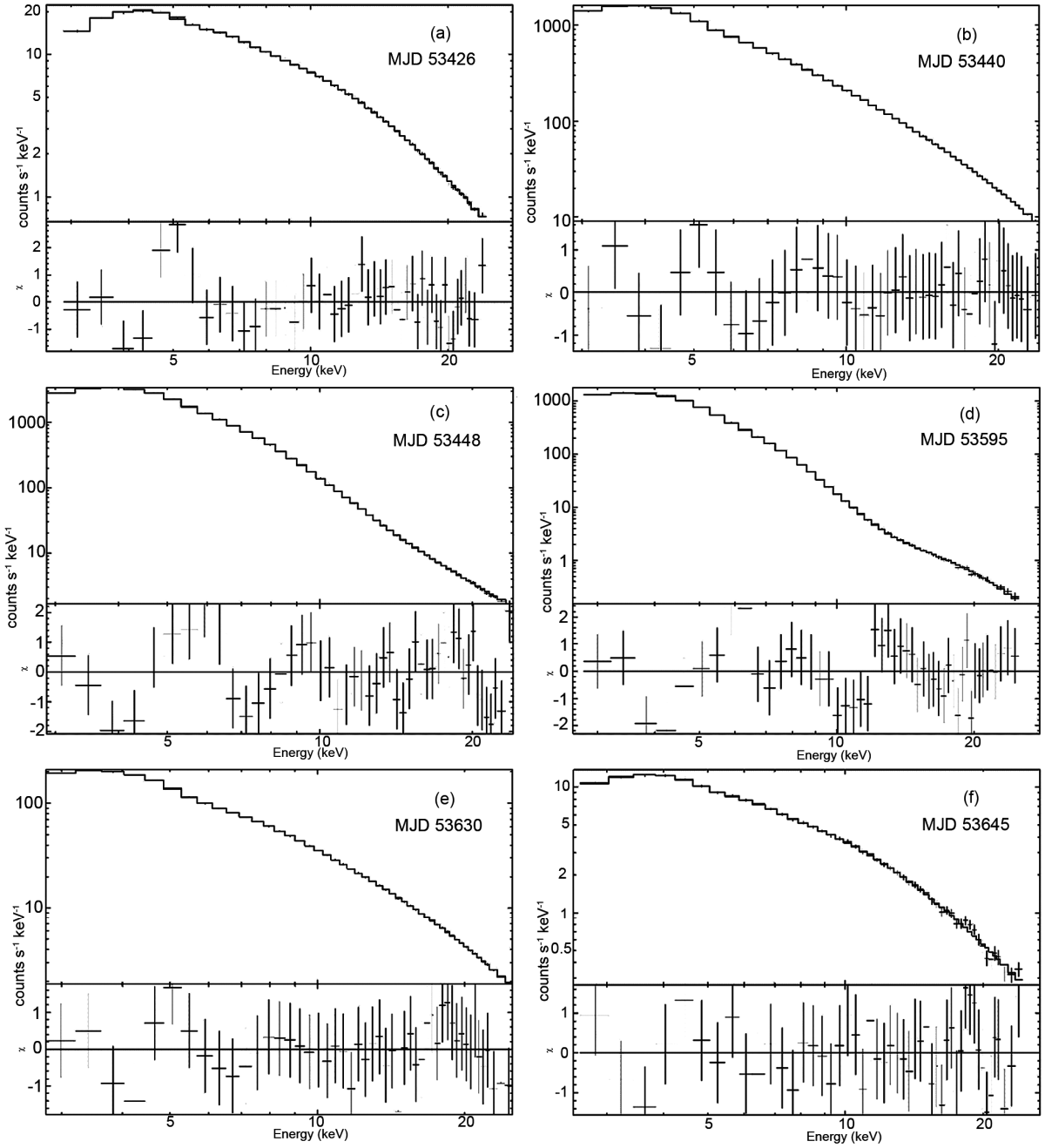

Fig. 4 — The TCAF model fitted 2.5 - 25 keV PCA spectra with variations of χ, selected from six different spectral states. The spectra of the rising phase are shown in the left panel, whereas the right panel show the spectra from the declining phase of the outburst. From top to bottom, the spectra show the hard, hard-intermediate, and soft-intermediate states

spectral states (hard, hard-intermediate, and soft-intermediate) during both the rising and declining phases. The figures show that the TCAF model provides a good fit for the hard and hard-intermediate spectra. Although the fit for the soft-intermediate state spectra is comparatively weaker, it remains acceptable, as indicated by the parameter values obtained from the fits.

4 Discussion

We presented a comprehensive analysis of the 2005 outburst of the Galactic transient black hole candidate, GRO J1655-40, using data obtained from the Rossi X-ray Timing Explorer (RXTE) mission. Our study focused on the temporal and spectral evolution of the source, employing the Two-Component Advective Flow (TCAF) model to gain insights into the accretion flow dynamics and the classification of spectral states.

From Fig. 1(a), we can see that during hard and hard-intermediate states in the rising phase of the outburst, the 5–15 keV photon count rate initially increases slowly in the hard state, then rapidly in the hard-intermediate state. On the other hand, from the hardness ratio plot of Fig. 1(b), it is seen that the hardness ratio of 9–15 to 5–8 keV photon count rates decreases at a faster rate in the hard-intermediate state than in the hard state. The reverse effect is seen during the declining phase of the outburst. The cause of the outburst could be attributed to changes in the physical characteristics of matter, particularly viscosity, possibly as a result of the increased magnetic activity. As the outburst builds momentum in the rising phase, increased viscosity facilitates a surge in the accretion rate of Keplerian matter. Subsequently, as viscosity decreases, the outburst subsides, leading to a reduction in the Keplerian rate and the recision of the disk. According to the Two-Component Advective Flow (TCAF) model, the initial phase of the outburst is characterized by a dominance of low angular-momentum sub-Keplerian flow, resulting in a hard/low-hard spectral state. As the outburst unfolds, the accretion rate within the Keplerian component intensifies, transitioning the object into a softer spectral state. Finally, during the declining phase of the outburst, the Keplerian flow retreats, while the rate of sub-Keplerian matter remains relatively constant, resulting in a spectral hardening.

We have presented the Hardness Intensity Diagram (HID) in Fig. 2 wherein the spectral state evolutions are depicted in a so-called q-diagram where PCA 5–15 keV count rate is plotted as a function of Hardness Ratio defined by the ratio of the flux in the 9–15 keV to that in the 5–8 keV energy band on logarithmic scale.This kind of presentation of HID in the form of so-called hysteresis loop can also be seen elsewhere[3,4,38] in the literature. But, as the definition of hardness intensity and the energy ranges used in the numerator and denominator are not unique and can be chosen arbitrarily[39], we believe that use of TCAF model for directly extracting the accretion parameters provides more physical and clear insight of what happens to the object during its outburst.

In Fig. 3(h), we have shown the variations of QPO frequencies with time (MJD) during the rising and declining phases of the outburst. QPOs are observed in the hard and hard-intermediate states – both in the rising and declining phases, while no QPO is seen in the soft-intermediate and soft states. Since shocks develop in hard and hard-intermediate states and the Compton cooling timescale is comparable to the in fall period from the shock to the inner edge of the disk, the prerequisites for the occurrence of QPO are easily met in these states. During the soft and soft-intermediate states, when the Keplerian rate is relatively higher, CENBOL experiences rapid cooling, and usually shocks are not formed. This is true in both the rising and declining phases. Eventually, no QPOs are seen in the soft-intermediate and soft states. In the rising phase, when going from hard state to hard-intermediate state, the halo rate increases while the disk rate remains almost steady, resulting in a rise in ARR. A similar thing happens in the declining phase when the source proceeds through hard-intermediate state to hard state. Consequently, there is a sharp peak in the ARR on the day of transition from the hard state to the hard-intermediate state during the rising phase, and conversely during the declining phase. This suggests a strong coupling between the occurrence of QPOs and the cooling characteristics of the disk. Nandi *et al.*[4] & Debnath *et al.*[38] found similar nature of variation of QPO frequency of compact objects during their outbursts and explained these variations using the propagating oscillation shock model. However, Akter *et al.*[34] presented HFQPOs of ~300Hz and ~450 Hz observed in GRO J1655-40 and explained their origin using their model constraining the range of black hole spin.

In Fig. 3 we have shown the variation of physical parameters like the disk and halo rates, accretion rate ratio, shock location and compression ratio during the 2005 outburst of GRO J1655-40. When an outburst is

triggered, the sub-Keplerian flow dominates in the accretion process since it moves faster with free-fall velocity due to lower viscosity and angular momentum than the Keplerian disk which moves in viscous time scale. The CENBOL truncates the Keplerian disk far away forming a shock at about hundred Schwarzschild radii (higher R) when the hard state (HS) is observed. During this period the sub-Keplerian halo rate dominates over the Keplerian disk rate and as a consequence ARR increases gradually. QPOs are produced due to resonance oscillation of the shock.

When the source enters into HIMS from HS, the halo rate decreases while the disk rate rises slowly resulting in a decrease in ARR. The rise in Keplerian disk rate makes the CENBOL cooler and the shock moves inward faster causing the CENBOL shrink. Here also QPOs are observed. The Compton cooling reduces the post-shock pressure and the shock strength reduces. The density of the post-shock matter decreases resulting in a decrease in compression ratio.

In the SIMS, more and more sub-Keplerian matter becomes Keplerian by viscous transport and as a result the Keplerian disk rate continues to rise. In this state, the soft X-ray flux increases while the hard X-ray flux reduces. The shock becomes very weak and the CENBOL becomes very small. No QPOs are seen in this state of GRO J1655-40.

In the soft state, only the Keplerian disk prevails completely cooling down the CENBOL. No shock is formed. No QPO is produced in the soft state.

During the declining phase of the outburst, the flow parameters undergo opposite evolutions. In this phase the ARR starts increasing as the object enters into HIMS from SIMS because here the halo rate increases while the disk rate decreases. The day corresponding to the maximum ARR indicates the spectral state transition from HIMS to HS in the declining phase.

5 Conclusion

The Two-Component Advective Flow (TCAF) model is used as a local model in XSPEC to categorize the entire 2005 outburst of GRO J1655-40 into four distinct spectral states: hard, hard-intermediate, soft-intermediate, and soft. Based on the spectral fit parameters, we have explained the flow dynamics and transitions from one spectral state to another during the outburst. We have observed that ARR plays an important role in determining the spectral state transitions. It reaches the maximum on the days of transition from HS to HIMS and vice versa during the rising and declining phases respectively. The increasing value of R indicates that the CENBOL reappears in the HIMS and the shock results in the observed QPOs. In the literature, we can find different attempts to explain the physical processes happening in the accretion disk during spectral state transitions, like the evolution of the power density spectrum involving disk blackbody and powerlaw components or the evolution of X-ray hardness intensity presented in a q-shaped HID. Earlier, after the inclusion of TCAF in *XSPEC*, several workers like Mondal *et al.*[39], Debnath *et al.*[36] & Bhattacharjee *et al.*[40] reported the analysis of the accretion flow dynamics of several black hole candidates during their outbursts with the TCAF model. We have also been motivated here to present the spectral class transitions of GRO J1655-40 during its 2005 outburst using the two component advective flow model and found that our results are consistent with the previous findings. Hence, we believe that the TCAF model is one of the best models as it can provide a detailed account of the accretion flow dynamics around a compact object during each of the observed spectral states.

References

1 Belloni T, Homan J, Casella P, van der Klis M, Nespoli E, Lewin W H G, Miller J M & Méndez M, *Astron Astrophys*, 440 (2005) 207.
2 Remillard R A & McClintock J E, *Annu Rev Astron Astrophys*, 44 (2006) 49.
3 Debnath D, Chakrabarti S K, Nandi A & Mandal S, *Bull Astron Soc India*, 36 (2008) 151.
4 Nandi A, Debnath D, Mandal S & Chakrabarti S K, *Astron Astrophys*, 542 (2012) 56.
5 Bari M W & Chatterjee A K, *Indian J Phys*, 87 (2013) 309.
6 Fender R P, Belloni T M & Gallo E, *MNRAS*, 355 (2004) 1105.
7 Homan J & Belloni T, *Astrophys Space Sci*, 300 (2005) 107.
8 Belloni T, *The Jet Paradigm: Lect Notes Phys*, 794 (2010) 53.
9 Belloni T, Colombo A P, Homan J, Campana S & van der Klis M, *Astron Astrophys*, 390 (2002) 199.
10 Titarchuk L, Shaposhnikov N & Arefiev V, *Astrophys J*, 660 (2007) 556.
11 Chatterjee A K, Bari M W & Choudhury A K, *Indian J Phys*, 82 (2008) 1429.
12 Rao A R, Agrawal P C, Paul B, Vahia M N & Yadav J S, *Astron Astrophys*, 330 (1998) 181.
13 Belloni T, Klein-Wolt M, Mendez M, van der Klis M & van Paradijs J, *Astron Astrophys*, 362 (2000) 691.
14 Naik S, Rao A R & Chakrabarti S K, *J Astrophys Astron*, 23 (2002) 213.
15 Chakrabarti S K, Nandi A, Choudhury A K & Chatterjee U, *Astrophys J*, 607 (2004) 406.
16 Chakrabarti S K, *Astron Astrophys*, 5 (2005) 33.
17 Chakrabarti S K, Nandi A, Chatterjee A K, Choudhury A K & Chatterjee U, *Astron Astrophys*, 431 (2005) 825.

18 Choudhury A K, Chatterjee A K & Nandi A, *Bull Astr Soc India*, 35 (2007) 41.
19 Choudhury A K, Chatterjee A K, Bari M W & Chakrabarti S K, *Proc 2nd Kolkata Conf Observat Evid Black Holes Universe (AIP, Kolkata, India)*, 1053 (2008) 161.
20 Banerjee A, Chakrabarti S K & Bhattacharjee A, *42nd COSPAR Scientific Assembly*, 42 (2018) E1.
21 Zhang S N, Harmon B A, Paciesas W S, Wilson C A & Fishman G J, *IAU Circ*, 6106 (1994) 1.
22 Harmon B A, Wilson C A, Zhang S N, Paciesas W S, Fishman G J, Hjellming R M, Rupen M P, Scott D M, Briggs M S & Rubin B C, *Nature*, 374 (1995) 703.
23 Hjellming R M & Rupen M P, *Nature*, 375 (1995) 464.
24 Orosz J A & Bailyn C D, *Astrophys J*, 477 (1997) 876.
25 Bailyn C D, Orosz J A, McClintock J E & Remillard R A, *Nature*, 378 (1995) 157.
26 Greene J, Bailyn C D & Orosz J A, *Astrophys J*, 554 (2001) 1290.
27 Markwardt C B & Swank J H, *ATel*, 414 (2005) 1.
28 Chakrabarti S K, Nandi A, Debnath D, Sarkar R & Datta B G, *Indian J Phys*, 79 (2005) 841.
29 Shaposhnikov N, Swank J, Shrader C R, Rupen M, Beckmann V, Markwardt C B & Smith D A, *Astrophys J*, 655 (2007) 434.
30 Chakrabarti S K &Titarchuk L G, *Astrophys J*, 455 (1995) 623.
31 Chakrabarti S K & Das S, *Mon Not R Astron Soc*, 349 (2004) 649.
32 Brocksopp C, McGowan K E, Krimm H, Godet O, Roming P, Mason K O, Gehrels N, Still M, Page K, Moretti A, Shrader C R, Campana S & Kennea J, *MNRAS*, 365 (2006) 1203.
33 Trigo D M, Parmar A N, Miller J, Kuulkers E &Caballero-Garcia M D, *Astron Astrophys*, 462 (2007) 657.
34 Aktar, Das S, Nandi A & Sreehari H, *J Astrophys Astron*, 39 (2018) 17.
35 Debnath D, Chakrabarti S K & Mondal S, *Mon Not R Astron Soc*, 440 (2014) 121.
36 Debnath D, Mondal S & Chakrabarti S K, *Mon Not R Astron Soc*, 447 (2015) 1984.
37 Chakrabarti S K, Debnath D, Nandi A & Pal P S, *Astron Astrophys*, 489 (2008) L41.
38 Debnath D, Chakrabarti S K & Nandi A, *Adv Space Res*, 52 (2013) 2143.
39 Mondal S, Debnath D & Chakrabarti S K, *Astrophys J,* 786 (2014) 6.
40 Bhattacharjee A, Banerjee I, Banerjee A, Debnath D & Chakrabarti S K, *Mon Not R Astron Soc*, 466 (2017) 1372.